**Original Article**
J Vet Sci 2016, 17(1), 13-20 · http://dx.doi.org/10.4142/jvs.2016.17.1.13

JVS

# Reduction of adult hippocampal neurogenesis is amplified by aluminum exposure in a model of type 2 diabetes

Sung Min Nam[1,2], Jong Whi Kim[1,2], Dae Young Yoo[1,2], Hyo Young Jung[1,2], Jung Hoon Choi[3], In Koo Hwang[1,2,4], Je Kyung Seong[1,2,4], Yeo Sung Yoon[1,2,4,*]

[1]*Department of Anatomy and Cell Biology, College of Veterinary Medicine,* [2]*BK21 PLUS Program for Creative Veterinary Science Research, and Research Institute for Veterinary Science, and* [4]*Korea Mouse Phenotyping Center, Seoul National University, Seoul 08826, Korea*
[3]*Department of Anatomy, College of Veterinary Medicine, Kangwon National University, Chuncheon 24341, Korea*

In this study, we investigated the effects of chronic aluminum (Al) exposure for 10 weeks on cell proliferation and neuroblast differentiation in the hippocampus of type 2 diabetic rats. Six-week-old Zucker diabetic fatty (ZDF) and Zucker lean control (ZLC) rats were selected and randomly divided into Al- and non-Al-groups. Al was administered via drinking water for 10 weeks, after which the animals were sacrificed at 16 weeks of age. ZDF rats in both Al- and non-Al-groups showed increases in body weight and blood glucose levels compared to ZLC rats. Al exposure did not significantly affect body weight, blood glucose levels or pancreatic β-cells and morphology of the pancreas in either ZLC or ZDF rats. However, exposure to Al reduced cell proliferation and neuroblast differentiation in both ZLC and ZDF rats. Exposure to Al resulted in poor development of the dendritic processes of neuroblasts in both ZLC and ZDF rats. Furthermore, onset and continuation of diabetes reduced cell proliferation and neuroblast differentiation, and Al exposure amplified reduction of these parameters. These results suggest that Al exposure via drinking water aggravates the impairment in hippocampal neurogenesis that is typically observed in type 2 diabetic animals.

**Keywords:** Zucker diabetic fatty rat, aluminum, diabetes, drinking water, neurogenesis

## Introduction

Obesity and subsequent hyperglycemia leads to insulin resistance, which is the major initiating factor leading to the onset of type 2 diabetes mellitus (T2DM). T2DM is rapidly increasing in prevalence, and this condition often underlies complications such as hypertension, atherosclerosis, angina, and stroke [3,20]. Attention has also begun to focus on T2DM induced cognitive impairment, including correlations with neurodegeneration [37]. Among neurodegenerative diseases, Alzheimer's disease (AD) is the leading cause of neurodegeneration, and higher morbidity has been observed in older patients with diabetes. Previous research has demonstrated that the induction of insulin resistance accelerated Alzheimer's like changes in the brain [26]. However, animal studies to elucidate the mechanisms underlying the correlation between T2DM and AD are still insufficient and more research is required.

Epidemiological studies have found that higher AD-associated morbidity is associated with regions with higher chances of aluminum (Al) exposure [12,29]. Nevertheless, the role of Al in AD is still unclear. Even if Al exposure is not the determining factor underlying AD, research supports that it is one risk factor. Additionally, Al was shown to induce dementia-like encephalopathy in uremic patients with dialysis treatment [7]. Al has also been found in amyloid plaques of AD patients [40]. Animal studies investigating the correlation between Al exposure and AD revealed that Al contributes to amyloidogenesis and accumulates in AD model animals [27,34]. The primary route of Al absorption is dietary, including in drinking water. Al exists in compound form, combined with other elements, and the concentration of Al in water is naturally low. However, acid rain and use of Al salts as coagulants in water treatment have elevated its levels in drinking water [36]. Once dissolved into drinking water, Al is more effectively absorbed into the body than Al contained in food because of Al-binding to food components [12].

The effects of Al exposure on the brain of T2DM model

Received 20 Oct. 2014, Revised 12 Dec. 2014, Accepted 30 Dec. 2014
*Corresponding author: Tel: +82-2-880-1264; Fax: +82-2-871-1752; E-mail: ysyoon@snu.ac.kr
pISSN 1229-845X
eISSN 1976-555X

animals have not previously been demonstrated. Uremic condition makes the body more susceptible to Al toxicity [7], and diabetes patients experience uremia in the late phase of the disease. However, Al toxicity in diabetes needs to be confirmed; therefore, this study was conducted to investigate the effects of Al exposure in a diabetic model animal. Zucker diabetic fatty (ZDF) rats, which were used in this study, are leptin receptor deficient and show insulin insufficiency from 7- to 8-weeks of age and develop typical aspects of T2DM from 12-weeks of age [11]. Mild cognitive impairments including memory loss have appeared as early clinical signs of AD [9,13]. Pennanen *et al*. [24] demonstrated that the brain pathology of AD starts early in the hippocampus and connected entorhinal cortex. Recently acquired memories are dependent on the hippocampus, and impairment of these memories is an early clinical indicator [19]. Specifically, formation of new memories is closely related to adult hippocampal neurogenesis [6]. Therefore, in the present study, we investigated the short-term effects of Al exposure before studying the long-term effects of Al exposure in ZDF ($Lepr^{fa/fa}$) and Zucker lean control (ZLC, $Lepr^{+/+}$) rats.

## Materials and Methods

### Experimental animals

Male and female heterozygous type ($Lepr^{fa/+}$) ZDF rats were acquired from Genetic Models (USA) and mated to each other to obtain homozygous ZDF and ZLC rats. Only male homozygous ZDF and ZLC rats were used in our study because female homozygous ZDF rats do not develop hyperglycemia and subsequent diabetes relative to age-matched male homozygous ZDF rats [5]. Animals were housed in a conventional state under adequate temperature (23°C) and humidity (60%) control with a 12-h light/12-h dark cycle, and free access to tap water and Purina 5008 diet were provided as recommended by Genetic Models (Purina Korea, Korea). The procedures for handling and caring of animals followed the NIH Guide for the Care and Use of Laboratory Animals issued by the Institute of Laboratory Animal Resources, USA, 1996, and the protocols employed in this study were approved by the Institutional Animal Care and Use Committee (IACUC) of Seoul National University (SNU-140219-1). All experiments were designed to minimize the number of animals used and their suffering.

### Genotyping of *Lepr*$^{fa}$ gene and experimental design

The genotype of the $Lepr^{fa}$ gene was determined as described in our previous study [14]. To investigate the effects of Al treatments on the adult hippocampal neurogenesis, ZDF and ZLC rats were randomly divided into vehicle-(ZDF), Al-treated (ZDF-Al) vehicle-(ZLC) and Al-treated (ZLC-Al) groups (n = 5 per group). Aluminum chloride (Sigma, USA) was dissolved in deionized water (pH 6.7) at 2,000 ppm. Al solution was provided as drinking water for rats from when they were 6 to 10 weeks old. This schedule was adopted because Al-induced brain dysfunction and accumulation at this concentration in previous studies [21,32]. All animals were euthanized at 16 weeks of age.

### Body weight and blood glucose levels

To confirm the effects of Al treatment on diabetic model animals, body weight and blood glucose (fed glucose) levels were measured on the last day of the experiment. To measure blood glucose level, blood was sampled in the morning (9:00 AM) by tail nick using a 27 G needle, then analyzed using a portable glucose monitor (ACCU-CHEK GO; Roche, Germany).

### Tissue processing and H&E staining

For histological staining, animals in each group were anesthetized with 30 mg/kg Zoletil 50 (Virbac, France), then perfused transcardially with 0.1 M phosphate-buffered saline (PBS; pH 7.4) followed by 4% paraformaldehyde in 0.1 M phosphate buffer (pH 7.4). The pancreas and brains were removed and post-fixed in the same fixative for 12 h. For insulin immunohistochemistry and H&E staining, pancreatic tissues were dehydrated with graded concentrations of alcohol and xylene for embedding in paraffin. Next, 4 μm-thick sections were serially cut using a microtome (Leica, Germany), then mounted onto silane-coated slides (Muto-glass, Japan). Pancreas sections were stained with H&E according to the general protocols. For immunohistochemical staining of neurogenic markers, brains were removed and trimmed, after which they were post-fixed in the same fixative for 12 h. The brain tissues were then cryoprotected by infiltration with 30% sucrose for 1 to 2 days. Following equilibration in 30% sucrose in PBS, the brains were serially cut on a freezing sliding microtome (Leica) into 30 μm-thick coronal sections. The sections were then collected into six-well plates containing PBS for further processing.

### Immunohistochemistry

To obtain accurate data, immunohistochemical staining was carefully conducted under the same conditions. For paraffin sections, three pancreatic tissue sections were selected for each animal. Sections were hydrated and placed in 400 mL jars filled with citrate buffer (pH 6.0), then heated in a microwave oven (Optiquick Compact; Moulinex, France) at a frequency of 2.45 GHz and 800 W power setting for antigen retrieval. After three heating cycles of 5 min each, slides were allowed to cool at room temperature and then washed in PBS. For brain, tissue sections were selected between −3.00 and −4.08 mm to the bregma in reference to the rat atlas for each animal [23]. Ten sections 90 μm apart from each other were collected and sequentially treated with 0.3% hydrogen peroxide ($H_2O_2$) in PBS for 30 min followed by 10% normal goat serum in 0.05 M PBS for 30 min. The sections were then incubated with diluted

guinea pig anti-insulin (1 : 200; Abcam, UK) for pancreas, and rabbit anti-Ki67 antibody (1 : 500; Abcam) or goat anti-DCX antibody (1 : 50; Santa Cruz Biotechnology, USA) for brain overnight at room temperature. Thereafter, sections were subsequently exposed to biotinylated goat anti-guinea pig IgG, goat anti-rabbit IgG or rabbit anti-goat IgG and streptavidin peroxidase complex (1 : 200; Vector, USA). Samples were subsequently visualized by reaction with 3,3'-diaminobenzidine tetrachloride (Sigma) in 0.1 M Tris-HCl buffer (pH 7.2) and mounted on gelatin-coated slides. The sections were mounted in toluene based-mounting medium (Richard-Allan Scientific; Thermo Scientific, USA) following dehydration.

The region of interest in the dentate gyrus was analyzed using an image analysis system. Images were calibrated into an array of 512 × 512 pixels corresponding to a dentate gyrus (40× primary magnification). The resolution of each pixel contained 256 gray levels. The intensity of DCX immunoreactivity was evaluated by means of a relative optical density (ROD), which was obtained after transforming the mean gray level using the formula: ROD = log (256/mean gray level). The ROD of the background was determined in unlabeled portions using ImageJ and the value was subtracted for correction, yielding high ROD values in the presence of preserved structures and low values after structural loss. The ROD ratio of was calibrated as a percentage. The number of Ki67- and DCX-positive cells in all groups was counted using an image analysis system equipped with a computer-based CCD camera (Optimas 6.5 software; CyberMetrics, USA).

Additionally, the total dendritic length of DCX-positive neuroblasts (20 $DCX^+$ neuroblasts per group) was measured using ImageJ 1.59 software (National Institute of Health, USA) with a NeuronJ plug-in.

### Statistical analysis

The data shown here represent the means of experiments performed for each experimental region. Differences among means were analyzed by two-way analysis of variance followed by Bonferroni post-tests to elucidate differences among groups using the GraphPad Prism 5.0 software (GraphPad Software, USA). A $p < 0.05$ was considered significant.

## Results

### Body weight and blood glucose levels

The body weights steadily increased with age for all groups. At 16 weeks, body weights were significantly different between ZLC and ZDF rats. However, there was no significant difference in that of rats in the non-Al and Al groups (panel A in Fig. 1).

At the end of the experiment (16 weeks of age), the blood glucose levels in the ZLC and ZLC-Al rats were 104.67 mg/dL and 104.25 mg/dL, respectively. However, blood glucose levels in the ZDF rats increased to 487.33 mg/dL and 419.33 mg/dL in ZDF and ZDF-Al rats, respectively. There was no significant difference in blood glucose levels between ZDF and ZDF-Al rats. There was also no significant difference in blood glucose level among ZLC groups by Al treatment (panel B in Fig. 1).

### Pancreatic histology

In the ZLC group, pancreatic islets were round and compact upon H&E staining (panel A in Fig. 2). In this group, insulin immunoreactive cells (β cells) were densely detected in the core and throughout the pancreatic islets (panel B in Fig. 2). No histological changes were observed in the ZLC-Al group, and β cells were distributed throughout the islets as in the ZLC group (panels C and D in Fig. 2). However, in the ZDF group, slight hypertrophy of the islets was observed and reduction of the β cells was transparent (panels E and F in Fig. 2). No histological differences were found in the ZDF-Al group and β cells were sparsely distributed in the islets (panels G and H in Fig. 2).

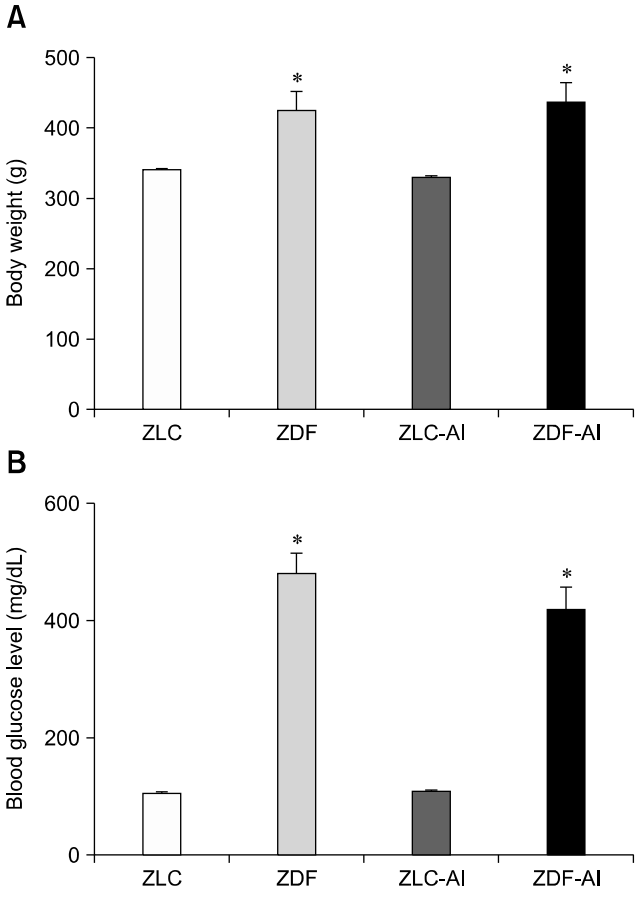


**Fig. 1.** Changes in body weight (A) and blood glucose levels (B) in vehicle-treated Zucker lean control (ZLC), vehicle-treated Zucker diabetic fatty (ZDF), aluminum-treated ZLC (ZLC-Al), and aluminum-treated ZDF (ZDF-Al) rats. Means were analyzed using two-way ANOVA ($n = 5$ per group; $*p < 0.05$, indicates a significant difference between ZLC and ZDF or ZLC-AL and ZDF-AL. Error bars indicate the means ± SEM.

### Effects of Al on cell proliferation in ZLC and ZDF rats

In the ZLC group, Ki67 immunoreactive nuclei were detected in the subgranular zone of the dentate gyrus (panels A and B in Fig. 3). In the ZLC-Al group, the number of Ki67 immunoreactive nuclei decreased to 56.50% of that observed in the ZLC group ($p < 0.001$) (panels C, D, and I in Fig. 3). Minimal Ki67 immunoreactive nuclei were found in tissue from the ZDF groups, and they were determined to be 35.01% of that of the ZLC group ($p < 0.001$) (panels E, F and I in Fig. 3). In the ZDF-Al group, Ki67 immunoreactive nuclei were rarely detected in the subgranular zone of the dentate gyrus and significantly reduced to 49.99% of the ZDF group (representing only 17.50% of the ZLC group) ($p < 0.05$) (panels G–I in Fig. 3). In the ZDF-Al group, their level was significantly reduced to

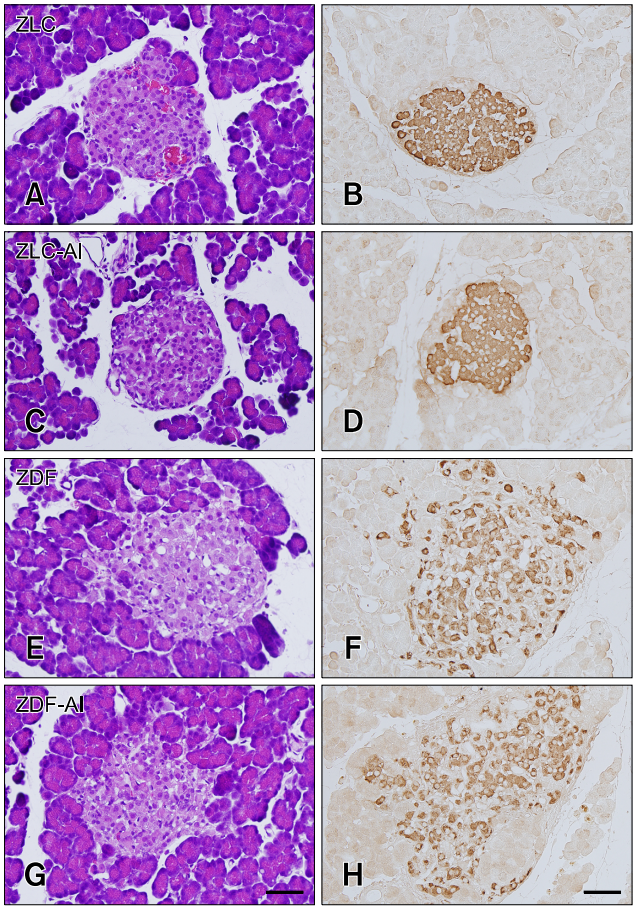


**Fig. 2.** Hematoxylin and eosin stain (A, C, E and G) and immunohistochemistry for insulin (B, D, F and H) of the pancreatic islets of the ZLC (A and B), ZLC-Al (C and D), ZDF (E and F), and ZDF-Al (G and H) groups. Note that the islets are slightly enlarged in the ZDF and ZDF-Al groups and insulin immunoreactive β cells are decreased in the ZDF and ZDF-Al groups. However, no histological and immunohistological differences were found between non-Al and Al groups. Scale bars = 50 μm.

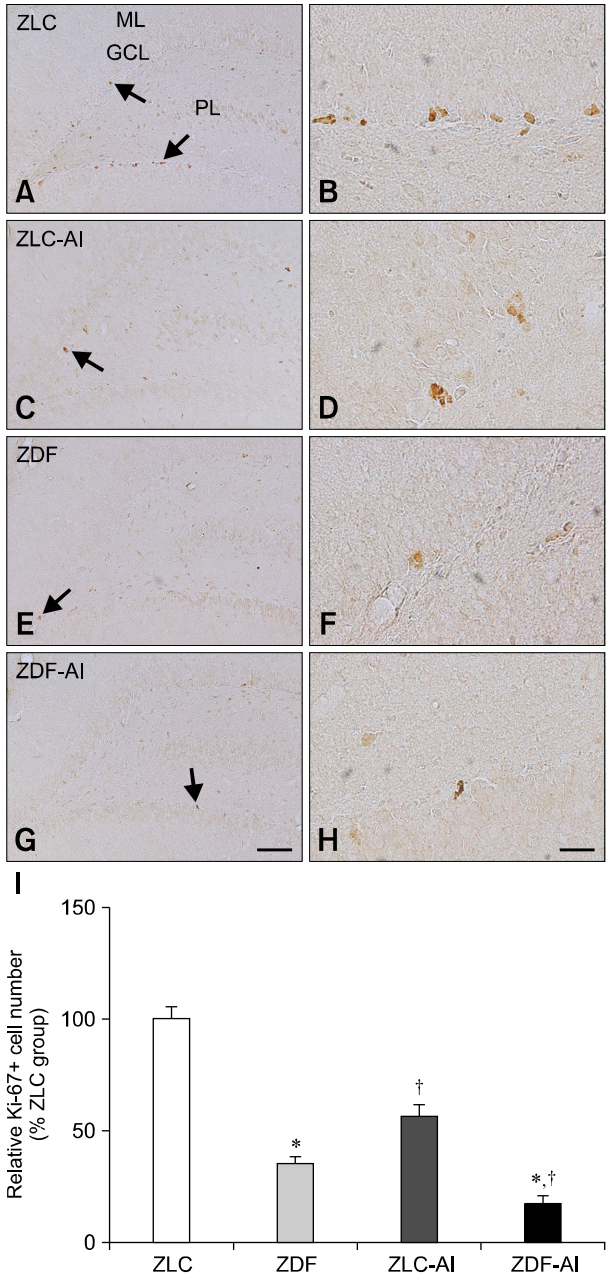


**Fig. 3.** Immunohistochemistry for Ki67 in the dentate gyrus of ZLC (A and B), ZLC-Al (C and D), ZDF (E and F), and ZDF-Al (G and H) groups. Ki67-immunoreactive nuclei were observed in the subgranular zone (arrows) of the dentate gyrus. Note that Ki67-immunoreactive nuclei are decreased in the ZLC-Al and ZDF-Al groups compared to the ZLC and ZDF groups, respectively. The lowest number of Ki67-immunoreactive nuclei was observed in the ZDF-Al group. (I) Relative mean number of Ki67-positive nuclei per section in all groups vs. ZLC group ($n = 5$ per group; $^{*}p < 0.05$, indicates a significant difference between ZLC and ZDF or ZLC-AL and ZDF-AL, $^{\dagger}p < 0.05$, indicates a significant difference between ZLC and ZLC-AL or ZDF and ZDF-AL). Error bars indicate the means ± SEM. Scale bars = 100 μm (A, C, E and G), 25 μm (B, D, F and H). GCL, granule cell layer; PL, polymorphic layer; ML, molecular layer.

30.97% of that in the ZLC-Al group ($p < 0.001$) (panel I in Fig. 3).

### Effects of Al on neuroblast differentiation in ZLC and ZDF rats

In all groups, cell bodies of DCX immunoreactive neuroblasts were located in the subgranular zone of the dentate gyrus, some of which were in the lower granule cell layer (Fig. 4). In the ZLC group, DCX immunoreactive neuroblasts were prominent among all groups, and well-developed dendrites with higher complexity were observed (panel A and in Fig. 4). The average dendritic length of DCX immunoreactive neuroblasts in this group was 468.21 μm (panel C in Fig. 5).

In the ZLC-Al group, the DCX immunoreactivity and number of DCX immunoreactive neuroblasts was reduced to 78.69% and 85.31% of the ZLC group, respectively ($p < 0.05$) (panels C and D in Fig. 4, and panels A and B in Fig. 5). The length of dendrites was decreased to 366.97 μm and the complexity of the

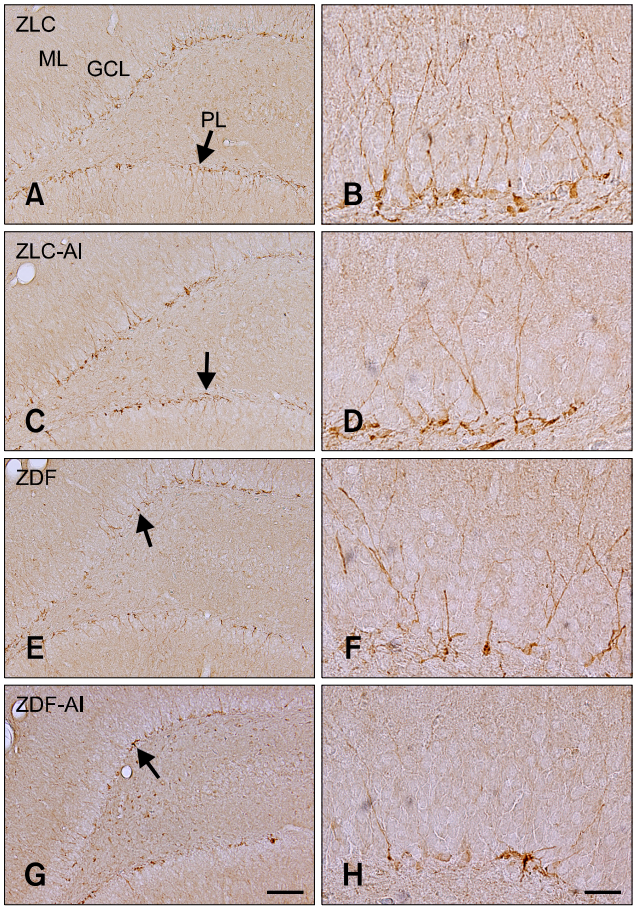


**Fig. 4.** Immunohistochemistry for DCX in the dentate gyrus of ZLC (A and B), ZLC-Al (C and D), ZDF (E and F), and ZDF-Al (G and H) groups. DCX-immunoreactive neuroblasts are observed in the subgranular zone (arrows) of the dentate gyrus. Note that DCX-immunoreactive neuroblasts were decreased in the ZLC-Al and ZDF-Al groups compared to the ZLC and ZDF groups, respectively. The lowest number of DCX-immunoreactive neuroblasts was observed in the ZDF-Al group. Scale bars = 100 μm (A, C, E and G), 25 μm (B, D, F and H).

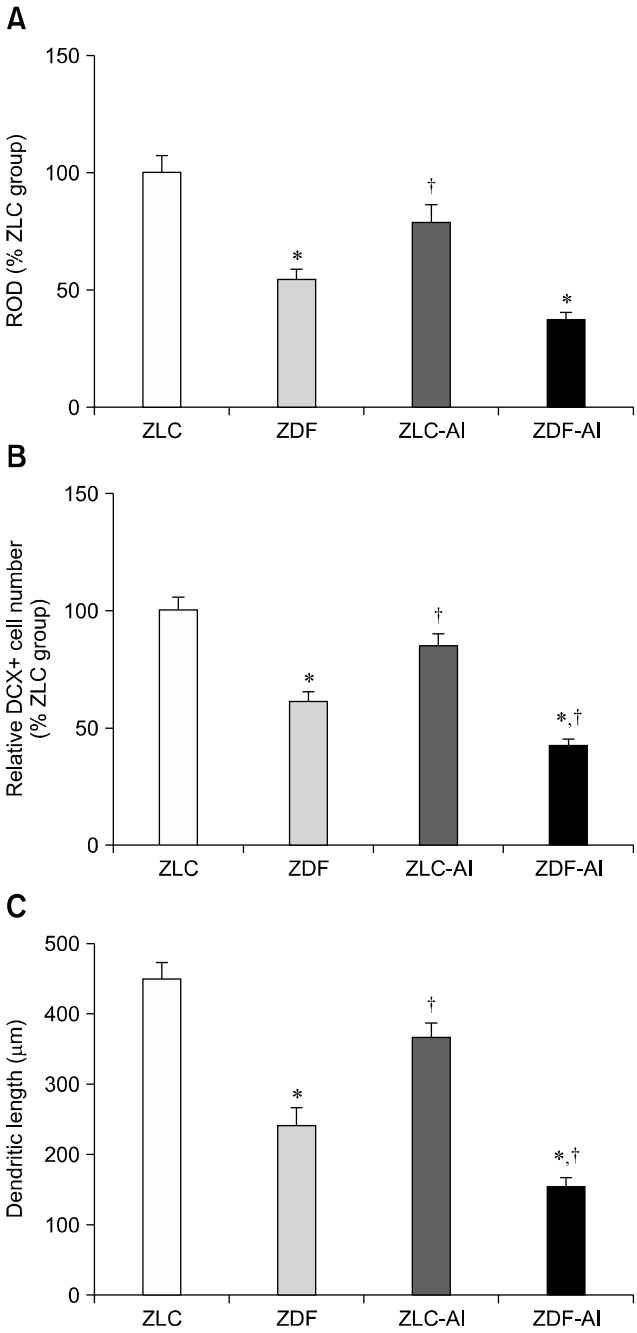


**Fig. 5.** Relative optical density (ROD) demonstrated as percentages of ZLC in DCX immunoreactivity (A), mean number of DCX-immunoreactive neuroblasts (B) and the length of neuroblast dendrites (C) in all groups ($n = 5$ per group; $n = 5$ per group; $^{*}p < 0.05$, indicates a significant difference between ZLC and ZDF or ZLC-AL and ZDF-AL, $^{\dagger}p < 0.05$, indicates a significant difference between ZLC and ZLC-AL or ZDF and ZDF-AL). Error bars indicate the means ± SEM.

dendritic branching was reduced in the ZLC-Al group ($p < 0.001$) (panels C and D in Fig. 4, and panel C in Fig. 5).

In the ZDF group, the DCX immunoreactivity and number of DCX immunoreactive cells was significantly reduced to 54.25% and 60.78% of those observed in the ZLC group, and the length of the dendrite was decreased to a mean of 248.86 μm ($p < 0.001$) (panels E and F in Fig. 4, and panels A–C in Fig. 5). In addition, dendritic branching was reduced relative to the ZLC group.

In the ZDF-Al group, the DCX immunoreactivity was reduced to 67.91% of that in the ZDF group (36.84% of that in the ZLC group) ($p > 0.05$), and most DCX immunoreactive neuroblasts in the ZDF-Al group had poorly-developed dendrites and decreased complexity of dendritic branching (panels G and H in Fig. 4, and panel A in Fig. 5). In addition, the lowest number (42.36% of that of the ZLC group) ($p < 0.05$) and the shortest dendrites (151.14 μm) of DCX immunoreactive neuroblasts were found in the ZDF-Al group ($p < 0.001$) (panels B and C in Fig. 5). In ZDF-Al group, the immunoreactivity, number and dendritic length was significantly reduced compared to those in the ZLC-Al group ($p < 0.001$) (panels A–C in Fig. 5).

## Discussion

ZDF rats, which are derived from Zucker obese rats, have a mutated leptin receptor that makes them obese and insulin resistant. Unlike the mild glucose intolerance observed in Zucker obese rats, ZDF rats develop severe glucose intolerance from the pre-diabetic phase through to the diabetic phase via insulin resistance with failure in pancreatic β cell mass compensation [25]. In previous studies, we found that the onset and continuation of the diabetic condition impaired cell proliferation and neuroblast differentiation in the hippocampal dentate gyrus [14]. In the present study, we investigated the effects of oral Al exposure from the pre-diabetic stage inT2DM rats on adult hippocampal neurogenesis.

First, we compared the physiological effects of diabetes and/or Al exposure in ZDF and ZLC rats at 16 weeks of age following a 10-week Al exposure period. ZDF rats showed significantly increased body weights and blood glucose levels. Even though the pattern of slight reduction in body weight and blood glucose levels was observed in ZDF-Al rats, this difference was not significant. In accordance with the past results [18,25], diabetic rats showed slight hypertrophy of the pancreatic islets and reduction of insulin immunoreactive β cells. However, Al exposure caused no significant difference in pancreatic histology or the distribution of β cells in this model. To the best of our knowledge, no studies have demonstrated the side effects of Al on the pancreas. In our previous study, intraperitoneal Al treatment resulted in the reduction of both blood glucose levels and body weight gain in mice with high fat diet induced obesity [22]. However, in the present study, exposure to Al via drinking water was not significantly associated with these parameters. The absorption rate for Al is dependent on the route of administration [7,30,39] and may explain the different results between our previous and present studies. Intraperitoneal Al administration produces more effective absorption and causes more Al accumulation in the brain than oral administration [30]. Exposure to Al as drinking water produces absorption rates of approximately 0.1 to 2.18% [7,39]. We selected drinking water as a route of Al ingestion because Al exposure via the intraperitoneal route is very rare in humans, whereas exposure to Al in drinking water is more probable. Additionally, lethality occurred after approximately 4 weeks of intraperitoneal injections, so we selected less lethal drinking water as a route of Al administration for our present study.

Next, we compared the effects of diabetes and/or Al exposure and found differences in cell proliferation and neuroblast differentiation between Al and non-Al groups. Similar to findings of previous studies of the effects of obesity and diabetes [14,22], type 2 diabetes impaired both cell proliferation and neuroblast differentiation in the present study. In addition, the total dendritic length of neuroblasts was significantly reduced by diabetes. High fat diet-induced obesity and type 2 diabetes induced cognitive malfunction, which is mediated by impairing functional and structural synaptic plasticity [31]. Impairment of both functional and structural hippocampal plasticity has also been reported in the hippocampus using a type 1 diabetic model [1,4]. Among many possible mechanisms of functional and structural hippocampal impairment in type 1 and 2 diabetes, hyperglycemia and increased glucocorticoid commonly exist and contributes to the development of neuropathology [4,31].

Exposure to Al impaired adult hippocampal neurogenesis in both ZLC and ZDF groups. However, Al treatment in diabetic rats exacerbated the reduction of cell proliferation and neuroblast differentiation. Along with reduction of the immunoreactivity and cell number, negative effects of Al on dendritic length and complexity of neuroblasts are apparent in both ZLC and ZDF rats. The results of our previous study are consistent with those of the present study because intraperitoneal Al treatment impaired adult hippocampal neurogenesis in mice with high fat diet-induced obesity [22]. DCX immunoreactive neuroblasts have an important role in learning [33]. In addition, synapse forming dendritic arborization of these neuroblasts was positively correlated with hippocampus-dependent spatial learning [38].

Al distributes to all regions of the brain, with the maximum concentration in the hippocampus [17]. After accumulation, Al develops neurotoxicity via several mechanisms, including oxidative stress, excitotoxicity, inflammation and apoptosis [2,10]. However, the mechanism of the Al neurotoxicity was not investigated in our present study. In other studies, Al

treatment induced functional deficits such as learning and memory impairment in mice and rats [16,28]. Along with reduction of adult hippocampal neurogenesis, intragastrically fed Al negatively affected ultrastructural configuration of the synapse [16]. In addition, chronic feeding of Al via drinking water impaired the synaptic plasticity (LTP and LDP) of the hippocampal dentate gyrus [35]. Long-term dietary Al accelerated amyloid peptide formation and plaque deposition in the transgenic model of Alzheimer's disease [27]. Ribes *et al*. [28] reported that, in this model, seven months of dietary Al exposure impaired spatial memory but spared cell proliferation and neuronal differentiation. There are three possible reasons for the absence of a significant difference in neurogenesis. Specifically, training and behavioral tests can increase hippocampal neurogenesis [8]. Additionally, the effects of the administrative form of Al in diet and water can be different for absorptive efficiency [12]. Finally, in the early stages of Alzheimer's disease, hippocampal neurogenesis increases as a compensatory mechanism for progressive neurodegeneration [15].

In conclusion, chronic exposure to Al via drinking water exacerbates the diabetes-induced reduction in cell proliferation and neuroblast differentiation.

## Acknowledgments

This research was supported by the Basic Science Research Program of the National Research Foundation (NRF) funded by the Korean government (MEST) (NRF-2012R1A1B3001256). This research was also supported by Korea Mouse Phenotyping Project (2013M3A9D5072550) of the Ministry of Science, ICT and Future Planning through NRF, Korea.

## Conflict of Interest

There is no conflict of interest.

## References

1. **Beauquis J, Saravia F, Coulaud J, Roig P, Dardenne M, Homo-Delarche F, De Nicola A.** Prominently decreased hippocampal neurogenesis in a spontaneous model of type 1 diabetes, the nonobese diabetic mouse. Exp Neurol 2008, **210**, 359-367.
2. **Becaria A, Lahiri DK, Bondy SC, Chen D, Hamadeh A, Li H, Taylor R, Campbell A.** Aluminum and copper in drinking water enhance inflammatory or oxidative events specifically in the brain. J Neuroimmunol 2006, **176**, 16-23.
3. **Beckman JA, Creager MA, Libby P.** Diabetes and atherosclerosis: epidemiology, pathophysiology, and management. JAMA 2002, **287**, 2570-2581.
4. **Biessels GJ, Kamal A, Ramakers GM, Urban IJ, Spruijt BM, Erkelens DW, Gispen WH.** Place learning and hippocampal synaptic plasticity in streptozotocin-induced diabetic rats. Diabetes 1996, **45**, 1259-1266.
5. **Corsetti JP, Sparks JD, Peterson RG, Smith RL, Sparks CE.** Effect of dietary fat on the development of non-insulin dependent diabetes mellitus in obese Zucker diabetic fatty male and female rats. Atherosclerosis 2000, **148**, 231-241.
6. **Deng W, Aimone JB, Gage FH.** New neurons and new memories: how does adult hippocampal neurogenesis affect learning and memory? Nat Rev Neurosci 2010, **11**, 339-350.
7. **DeVoto E, Yokel RA.** The biological speciation and toxicokinetics of aluminum. Environ Health Perspect 1994, **102**, 940-951.
8. **Döbrössy MD, Drapeau E, Aurousseau C, Le Moal M, Piazza PV, Abrous DN.** Differential effects of learning on neurogenesis: learning increases or decreases the number of newly born cells depending on their birth date. Mol Psychiatry 2003, **8**, 974-982.
9. **Dubois B, Albert ML.** Amnestic MCI or prodromal Alzheimer's disease? Lancet Neurol 2004, **3**, 246-248.
10. **El-Rahman SS.** Neuropathology of aluminum toxicity in rats (glutamate and GABA impairment). Pharmacol Res 2003, **47**, 189-194.
11. **Etgen GJ, Oldham BA.** Profiling of Zucker diabetic fatty rats in their progression to the overt diabetic state. Metabolism 2000, **49**, 684-688.
12. **Flaten TP.** Aluminium as a risk factor in Alzheimer's disease, with emphasis on drinking water. Brain Res Bull 2001, **55**, 187-196.
13. **Helkala EL, Laulumaa V, Soininen H, Riekkinen PJ.** Recall and recognition memory in patients with Alzheimer's and Parkinson's diseases. Ann Neurol 1988, **24**, 214-217.
14. **Hwang IK, Yi SS, Song W, Won MH, Yoon YS, Seong JK.** Effects of age and treadmill exercise in chronic diabetic stages on neuronal differentiation in a rat model of type 2 diabetes. Brain Res 2010, **1341**, 63-71.
15. **Jin K, Peel AL, Mao XO, Xie L, Cottrell BA, Henshall DC, Greenberg DA.** Increased hippocampal neurogenesis in Alzheimer's disease. Proc Natl Acad Sci U S A 2004, **101**, 343-347.
16. **Jing Y, Wang Z, Song Y.** Quantitative study of aluminum-induced changes in synaptic ultrastructure in rats. Synapse 2004, **52**, 292-298.
17. **Julka D, Vasishta RK, Gill KD.** Distribution of aluminum in different brain regions and body organs of rat. Biol Trace Elem Res 1996, **52**, 181-192.
18. **Kakimoto T, Kimata H, Iwasaki S, Fukunari A, Utsumi H.** Automated recognition and quantification of pancreatic islets in Zucker diabetic fatty rats treated with exendin-4. J Endocrinol 2013, **216**, 13-20.
19. **Kitamura T, Inokuchi K.** Role of adult neurogenesis in hippocampal-cortical memory consolidation. Mol Brain 2014, **7**, 13.
20. **Luitse MJA, Biessels GJ, Rutten GEHM, Kappelle LJ.** Diabetes, hyperglycaemia, and acute ischaemic stroke. Lancet Neurol 2012, **11**, 261-271.
21. **Luo Y, Nie J, Gong QH, Lu YF, Wu Q, Shi JS.** Protective effects of icariin against learning and memory deficits induced by aluminium in rats. Clin Exp Pharmacol Physiol 2007, **34**, 792-795.

22. **Nam SM, Kim JW, Yoo DY, Kim W, Jung HY, Hwang IK, Seong JK, Yoon YS.** Additive or synergistic effects of aluminum on the reduction of neural stem cells, cell proliferation, and neuroblast differentiation in the dentate gyrus of high-fat diet-fed mice. Biol Trace Elem Res 2014, **157**, 51-59.
23. **Paxinos G, Watson C.** The Rat Brain in Stereotaxic Coordinates. 6th ed. Academic Press, Amsterdam, 2007.
24. **Pennanen C, Kivipelto M, Tuomainen S, Hartikainen P, Hänninen T, Laakso MP, Hallikainen M, Vanhanen M, Nissinen A, Helkala EL, Vainio P, Vanninen R, Partanen K, Soininen H.** Hippocampus and entorhinal cortex in mild cognitive impairment and early AD. Neurobiol Aging 2004, **25**, 303-310.
25. **Pick A, Clark J, Kubstrup C, Levisetti M, Pugh W, Bonner-Weir S, Polonsky KS.** Role of apoptosis in failure of beta-cell mass compensation for insulin resistance and beta-cell defects in the male Zucker diabetic fatty rat. Diabetes 1998, **47**, 358-364.
26. **Plaschke K, Kopitz J, Siegelin M, Schliebs R, Salkovic-Petrisic M, Riederer P, Hoyer S.** Insulin-resistant brain state after intracerebroventricular streptozotocin injection exacerbates Alzheimer-like changes in Tg2576 AβPP-overexpressing mice. J Alzheimers Dis 2010, **19**, 691-704.
27. **Praticò D, Uryu K, Sung S, Tang S, Trojanowski JQ, Lee VM.** Aluminum modulates brain amyloidosis through oxidative stress in APP transgenic mice. FASEB J 2002, **16**, 1138-1140.
28. **Ribes D, Colomina MT, Vicens P, Domingo JL.** Impaired spatial learning and unaltered neurogenesis in a transgenic model of Alzheimer's disease after oral aluminum exposure. Curr Alzheimer Res 2010, **7**, 401-408.
29. **Rondeau V, Jacqmin-Gadda H, Commenges D, Helmer C, Dartigues JF.** Aluminum and silica in drinking water and the risk of Alzheimer's disease or cognitive decline: findings from 15-year follow-up of the PAQUID cohort. Am J Epidemiol 2009, **169**, 489-496.
30. **Sánchez-Iglesias S, Soto-Otero R, Iglesias-González J, Barciela-Alonso MC, Bermejo-Barrera P, Méndez-Alvarez E.** Analysis of brain regional distribution of aluminium in rats via oral and intraperitoneal administration. J Trace Elem Med Biol 2007, **21** (Suppl 1), 31-34.
31. **Stranahan AM, Arumugam TV, Cutler RG, Lee K, Egan JM, Mattson MP.** Diabetes impairs hippocampal function through glucocorticoid-mediated effects on new and mature neurons. Nat Neurosci 2008, **11**, 309-317.
32. **Van Alstyne R, McDowell LR, Davis PA, Wilkinson NS, O'Connor GA.** Effects of an aluminum-water treatment residual on performance and mineral status of feeder lambs. Small Rumin Res 2007, **73**, 77-86.
33. **Vukovic J, Borlikova GG, Ruitenberg MJ, Robinson GJ, Sullivan RKP, Walker TL, Bartlett PF.** Immature doublecortin-positive hippocampal neurons are important for learning but not for remembering. J Neurosci 2013, **33**, 6603-6613.
34. **Walton JR, Wang MX.** APP expression, distribution and accumulation are altered by aluminum in a rodent model for Alzheimer's disease. J Inorg Biochem 2009, **103**, 1548-1554.
35. **Wang M, Chen JT, Ruan DY, Xu YZ.** Vasopressin reverses aluminum-induced impairment of synaptic plasticity in the rat dentate gyrus in vivo. Brain Res 2001, **899**, 193-200.
36. **World Health Organization.** Aluminium. In: Guidelines for Drinking-water Quality. 2nd ed. Addendum to Vol. 2. Health criteria and other supporting information. World Health Organization, Geneva, 1998.
37. **Xu W, Caracciolo B, Wang HX, Winblad B, Bäckman L, Qiu C, Fratiglioni L.** Accelerated progression from mild cognitive impairment to dementia in people with diabetes. Diabetes 2010, **59**, 2928-2935.
38. **Yau SY, Lau BW, Tong JB, Wong R, Ching YP, Qiu G, Tang SW, Lee TM, So KF.** Hippocampal neurogenesis and dendritic plasticity support running-improved spatial learning and depression-like behaviour in stressed rats. PLoS One 2011, **6**, e24263.
39. **Yokel RA, McNamara PJ.** Influence of renal impairment, chemical form, and serum protein binding on intravenous and oral aluminum kinetics in the rabbit. Toxicol Appl Pharmacol 1988, **95**, 32-43.
40. **Yumoto S, Kakimi S, Ohsaki A, Ishikawa A.** Demonstration of aluminum in amyloid fibers in the cores of senile plaques in the brains of patients with Alzheimer's disease. J Inorg Biochem 2009, **103**, 1579-1584.